DALTON
FULL PAPER

Dinuclear ruthenium(II) complexes as probes for DNA bulge sites †

Bradley T. Patterson,[a] J. Grant Collins,*[b] Fiona M. Foley[a] and F. Richard Keene*[a]

[a] *School of Pharmacy & Molecular Sciences, James Cook University, Townsville, Queensland 4811, Australia. E-mail: Richard.Keene@jcu.edu.au*
[b] *School of Chemistry, University College, University of New South Wales, Australian Defence Force Academy, Canberra, A.C.T. 2600, Australia. E-mail: g-collins@adfa.edu.au*

Received 16th August 2002, Accepted 2nd October 2002
First published as an Advance Article on the web 4th November 2002

The binding of the dinuclear ruthenium(II) complexes ΔΔ-[{Ru(Me_2bpy)$_2$}$_2$(μ-bpm)]$^{4+}$ and ΔΔ-[{Ru(bpy)$_2$}(μ-bpm)-{Ru(Me_2bpy)$_2$}]$^{4+}$ {bpy = 2,2′-bipyridine; Me_2bpy = 4,4′-dimethyl-2,2′-bipyridine; bpm = 2,2′-bipyrimidine} to a tridecanucleotide containing a single adenine bulge has been studied by ^{1}H NMR spectroscopy. The addition of either complex to d(CCGAGAATTCCGG)$_2$ induced significant chemical shift changes for the base and sugar resonances of the residues at the bulge site ($G_3A_4G_5/C_{11}C_{10}$). In NOESY spectra of the tridecanucleotide bound with either ruthenium species, NOEs were observed from the H1′ and H4′ protons of the nucleotide residues at the bulge site to the Me_2bpy and bpm protons of the metal complex. These results indicate that the dinuclear ruthenium species selectively bind at the adenine bulge site in the minor groove. A simple model was constructed for the binding of the non-symmetrical ΔΔ-[{Ru(bpy)$_2$}(μ-bpm){Ru(Me_2bpy)$_2$}]$^{4+}$ complex, which shows that the minor groove has significantly widened to allow the relatively bulky complex to bind. As the metal complexes specifically bind at an adenine bulge site in a segment of DNA with an affinity considerably greater than that for standard duplex DNA, the results presented here suggest that non-intercalating dinuclear complexes may be excellent diagnostic agents for DNA bulged sequences.

Introduction

Although considerable attention has been devoted over the last decade to mononuclear ruthenium(II) complexes that bind to DNA by intercalation,[1–3] there is growing interest in the DNA binding of polypyridyl-based dinuclear ruthenium(II) complexes.[4–9] These dinuclear complexes can bind DNA by bis-intercalation,[4] or associate as positively-charged species within the grooves of polyanionic DNA.[5–9] While the binding with intercalating complexes is strong, it has been shown that when intercalation is not involved in relatively bulky dinuclear ruthenium(II) complexes such as [{Ru(phen)$_2$}$_2$(μ-HAT)]$^{4+}$ {HAT = 1,4,5,8,9,12-hexaazaphenylene}, they interact with double-stranded DNA only weakly.[8] In a recent NMR study of the binding of [{Ru(Me_2bpy)$_2$}$_2$(μ-bpm)]$^{4+}$ {Me_2bpy = 4,4′-dimethyl-2,2′-bipyridine; bpm = 2,2′-bipyrimidine} to two dodecanucleotides, we found that despite the bulk of the metal complex it bound preferentially in the DNA minor groove, but with relatively low affinity.[10]

However, the binding of such complexes to partially-denatured DNA is relatively strong.[8] Consequently, while the bulky dinuclear complexes cannot bind deeply within the DNA minor groove, they may preferentially bind DNA structures that are more open—such as partially-denatured DNA. One example of a biologically important open structure is a sequence that contains a DNA bulge. Unpaired or base bulges occur where the duplex section of the DNA helix is interrupted by the inclusion on one strand of one or more bases that have no base(s) on the complementary strand with which to form a base-pair.[11] Bulged bases are thought to play an important role in frame-shift mutagensis and are a specific recognition site for various DNA binding proteins.[11] Given the importance of DNA bulges in biological systems, there has been considerable recent interest in developing small molecules that can specifically bind to them.[12–14]

Herein we present the results of a NMR study of the interaction of two dinuclear ruthenium complexes, ΔΔ-[{Ru(Me_2bpy)$_2$}$_2$(μ-bpm)]$^{4+}$ and ΔΔ-[{Ru(bpy)$_2$}(μ-bpm)-{Ru(Me_2bpy)$_2$}]$^{4+}$ (see Fig. 1A), to a tridecanucleotide

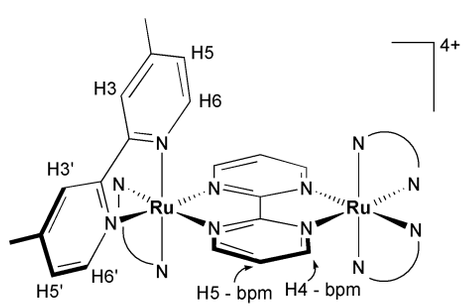

Fig. 1 The structure and atom numbering of ΔΔ-[{Ru(Me_2bpy)$_2$}$_2$-(μ-bpm)]$^{4+}$ and a structural representation of the adenine bulge (A_4) containing tridecanucleotide (B).

d(CCGAGAATTCCGG)$_2$ that contains a single adenine bulge (see Fig. 1B). This particular oligonucleotide was chosen in this work because a previous NMR study of its conformation in solution demonstrated that it adopted a double helix with the extra adenine (A_4) being accommodated within the helix.[15]

Initially, NMR experiments were carried out using the symmetric [{Ru(Me_2bpy)$_2$}$_2$(μ-bpm)]$^{4+}$ species because its binding to two dodecanucleotides, d(CAATCCGGATTG)$_2$ and d(CAATCGCGATTG)$_2$, has been previously characterised.[10,16]

† Electronic supplementary information (ESI) available: CD spectra of the enantiomers of [{Ru(bpy)$_2$}(μ-bpm){Ru(Me_2bpy)$_2$}]$^{4+}$. See http://www.rsc.org/suppdata/dt/b2/b208047h/

For the former dodecanucleotide the metal complex bound at the CCGG site with an association constant of 3×10^3 M^{-1}, while for the latter the metal complex bound at the AAT site with an association constant of 1×10^4 M^{-1}. In order for a simple binding model to be proposed, subsequent binding experiments were carried out using the non-symmetric [{Ru(bpy)$_2$}(μ-bpm){Ru(Me$_2$bpy)$_2$}]$^{4+}$ species, where it is possible to distinguish between the two ruthenium centres in the free and tridecanucleotide-bound dinuclear complex. The NMR data indicate that the dinuclear ruthenium(II) complexes specifically bind at the bulged site with an affinity considerably higher than that determined for the corresponding non-bulged oligonucleotide and that previously determined for other standard duplex oligonucleotides.[10]

Experimental

Physical measurements

Circular dichroism (CD) spectra were recorded in acetonitrile solution at concentrations of *ca.* 2–3 × 10^{-5} M in a 0.1 dm cell, using a JASCO J-715 spectropolarimeter. CD spectra have been corrected for concentration and are presented as Δε (dm^3 mol^{-1} cm^{-1}) *vs.* wavelength, λ (nm). Electronic spectra were recorded using a Cary 5E UV/Vis/NIR spectrophotometer. 1D and 2D ^{1}H NMR spectra used in association with the synthetic studies were performed on a Varian Mercury 300 MHz spectrometer, and chemical shifts reported relative to 99.9% d$_3$-acetonitrile (CD$_3$CN, δ = 1.93 ppm) unless otherwise specified. For the DNA binding studies, NMR experiments were recorded on a Varian Unityplus-400 NMR spectrometer, operating at 400 MHz for the ^{1}H nuclei.

Materials

2-Methoxyethanol (Aldrich), potassium hexafluorophosphate (KPF_6; Aldrich), and trimethyl-*N*-oxide hydrate (TMNO; Fluka) were used as supplied. Solutions of sodium (−)-*O*,*O*′-dibenzoyl-L-tartrate and (−)-di-*O*,*O*′-4-toluoyl-L-tartrate were produced by neutralisation of the corresponding acids (Fluka) using NaOH. SP Sephadex C-25 used for chromatographic purification of ruthenium complexes[17] and CM Sephadex were obtained from Amersham Biosciences. Reagent solvents were used without further purification unless otherwise specified. Acetonitrile (CH_3CN; Aldrich; HPLC grade) was used for circular dichroism measurements.

The two self-complementary oligonucleotides d(CCGGAATTCCGG) and d(CCGAGAATTCCGG) were obtained from GeneWorks, South Australia. The complexes [Ru(Me$_2$bpy)$_2$(CO)$_2$](PF$_6$)$_2$,[18] [Ru(bpy)$_2$(bpm)](PF$_6$)$_2$[18] and ΔΔ-[{Ru(Me$_2$bpy)$_2$}$_2$(μ-bpm)](PF$_6$)$_4$[10,16] were synthesised as described previously.

Synthesis of ΔΔ-[{Ru(bpy)$_2$(μ-bpm){Ru(Me$_2$bpy)$_2$}]$^{4+}$

[{Ru(bpy)$_2$}(μ-bpm){Ru(Me$_2$bpy)$_2$}](PF$_6$)$_4$. *rac*-[Ru(bpy)$_2$(bpm)](PF$_6$)$_2$ (100 mg, 0.12 mmol) and *rac*-[Ru(Me$_2$bpy)$_2$(CO)$_2$](PF$_6$)$_2$ (180 mg, 0.22 mmol) were combined in 2-methoxyethanol (50 cm^3) and sparged with N_2 for 15 min. Trimethyl-*N*-oxide hydrate (TMNO; 0.88 mmol) was added and the temperature increased to 120 °C for 3.5 h. The mixture was diluted to 200 cm^3 with water and purified using cation-exchange chromatography (SP Sephadex C-25) with 0.4 M NaCl solution. The major green band was collected, precipitated with saturated KPF_6 solution and collected by filtration. Yield 188 mg (98%).

Separation of the diastereoisomers of [{Ru(bpy)$_2$}(μ-bpm){Ru(Me$_2$bpy)$_2$}]$^{4+}$. The complex was converted to the Cl^- salt by stirring an aqueous suspension of the PF_6^- salt with anion exchange resin (Cl^- form). After filtering and loading onto a cation-exchange column (SP Sephadex C-25) and elution with 0.15 M sodium (−)-*O*,*O*′-dibenzoyl-L-tartrate solution, the "*meso*" form (ΔΛ/ΛΔ) was separated within 40 cm and was collected after 1 m. The trailing *rac* band (ΔΔ/ΛΛ) was left to recycle on the column to resolve the two enantiomers. Resolution occurred with an "effective column length" of 2 m and the two bands (ΔΔ and ΛΛ) collected after 3 m of travel. Recovery of the products was achieved by the addition of aqueous KPF_6 solution to the eluted bands, followed by extraction with dichloromethane. In each case the organic layer was dried (Na_2SO_4) and the dichloromethane removed by rotary evaporation. ^{1}H NMR (CD_3CN—B indicates protons associated with the bpy ligand, D with Me$_2$bpy and M with bpm): "*meso*-": δ 2.53 (s, 6H, D4), 2.54 (s, 6H, D4), 7.27 (ddd, *J* = 5.7, 1.8, 0.7 Hz, 2H, D5), 7.40 (t, *J* = 5.7 Hz, 2H, M5), 7.41 (dd, *J* = 5.7, 1.8 Hz, 2H, D5), 7.44 (ddd, *J* = 7.5, 5.4, 1.2 Hz, 2H, B5), 7.47 (d, *J* = 6 Hz, 2H, D6), 7.60 (ddd, *J* = 7.5, 5.4, 1.2 Hz, 2H, B5), 7.68 (ddd, *J* = 5.7, 1.4, 0.7 Hz, 2H, B6), 7.81 (d, *J* = 6 Hz, 2H, D6), 7.98 (ABX coupling between M4 and M6, 4H, M4), 8.02 (ddd, *J* = 5.7, 1.4, 0.7 Hz, 2H, B6), 8.08 (td, *J* = 6.9, ~1 Hz, 2H, B4), 8.10 (td, *J* = 6.9, ~1 Hz, 2H, B4), 8.30 (dd, *J* = 1.1, 0.7 Hz, 2H, D3), 8.32 (dd, *J* = 1.1, 0.7 Hz, 2H, D3), 8.45 (dt, *J* = 8.6, ~1 Hz, 2H, B3), 8.48 (dt, *J* = 8.6, ~1 Hz, 2H, B3). *rac*-: δ 2.54 (s, 6H, D4), 2.61 (s, 6H, D4), 7.21 (dd, *J* = 5.7, 1.8 Hz, 2H, D5), 7.24 (dd, *J* = 5.7, 1.8 Hz, 2H, D5), 7.40 (t, *J* = 5.7, 2H, M5), 7.41 (ddd, *J* = 7.5, 5.4, 1.2 Hz, 2H, B5), 7.42 (d, *J* = 6 Hz, 2H, D6), 7.42 (ddd, *J* = 7.5, 5.4, 1.2 Hz, 2H, B5), 7.54 (d, *J* = 6 Hz, 2H, D6), 7.62 (ddd, *J* = 5.7, 1.4, 0.7 Hz, 2H, B6), 7.75 (ddd, *J* = 5.7, 1.4, 0.7 Hz, 2H, B6), 8.03 (ABX coupling between M4 and M6, 4H, M4), 8.08 (td, *J* = 6.9, ~1 Hz, 2H, B4), 8.19 (td, *J* = 6.9, ~1 Hz, 2H, B4), 8.36 (dd, *J* = 1.1, 0.7 Hz, 2H, D3), 8.38 (dd, *J* = 1.1, 0.7 Hz, 2H, D3), 8.52 (dt, *J* = 8.6, ~1 Hz, 2H, B3), 8.54 (dt, *J* = 8.6, ~1 Hz, 2H, B3). CD {λ/nm {Δε (ΔΔ, ΛΛ)}, CH_3CN}: 210 (−66.1, 66.1), 255 (58.5, −60.3), 279 (−146.8, 147.5), 319 (−43.9, 44.4), 389 (29.3, −28.7).

Sample preparation for NMR analysis

The oligonucleotides, which were obtained as tetraethylammonium salts, were converted to the sodium salt using a CM-Sephadex column that had been equilibrated with 1 M NaCl. After elution from the column, 650 μL of phosphate buffer (pH 7.0) containing 20 mM NaCl and 1 mM Na_2H_2EDTA were added and the solution freeze-dried. The oligonucleotide was then freeze-dried twice more from D_2O, and finally dissolved in 650 μL of 99.96% D_2O just prior to use. The concentration of the oligonucleotides were determined from the A_{260} absorbance, using an extinction coefficient of 6600 M^{-1} cm^{-1} per nucleotide.[19] Stock solutions of the metal complexes (15 mM) were prepared in D_2O. Additions of the metal complex stock solutions were made directly to the oligonucleotide solutions.

NMR Spectroscopy

All NMR experiments were recorded at 400 MHz for the ^{1}H nuclei (see above). Phase-sensitive NOESY spectra were acquired by the method of States *et al.*,[20] using 2048 data points in t_2 for 256 t_1 values with a pulse repetition delay of 1.7 s for mixing times ranging from 100 to 350 ms. DQFCOSY spectra were recorded using 2048 data points in t_2 for 256 t_1 values and a pulse repetition delay of 1.7 s. Two-dimensional NMR data sets were zero-filled to 1024 points in the t_1 dimension and apodized with either a Gaussian or a shifted sinebell function. One-dimensional spectra recorded in 90% H_2O/10% D_2O solution were collected using the WATERGATE solvent suppression technique of Piotto *et al.*[21]

Determination of binding constant

The association constant for the binding of the metal complex to an oligonucleotide can be expressed as:

$$K_{ass} = \frac{[\text{M-DNA}]}{[\text{M}][\text{DNA}]}$$

where [M-DNA] is the concentration of the metal complex-bound oligonucleotide and [DNA] and [M] are the concentrations of the free oligonucleotide and metal complex respectively. [M-DNA], [M] and [DNA] in the above equation can be estimated from the following equation and the initial concentrations of the metal complex and dodecanucleotide.[22]

$$\delta_{obs} = \chi_f\delta_f + \chi_b\delta_b$$

δ_{obs} is the observed chemical shift of the metal complex resonances, χ_f and χ_b are the mole fractions of free and bound metal complex and δ_f and δ_b are the chemical shifts of the resonances of the free and bound metal complex. The value for δ_b is taken from the shift at the lowest ratio of metal complex to oligonucleotide that the resonance can be assigned, while the value for δ_f is taken from the spectrum of the free metal complex in the identical buffer.

Binding model

The tridecanucleotide containing the bulge was constructed using HyperChem molecular modelling software.[23] The metal complex was manually docked in the tridecanucleotide minor groove at the bulge site and then energy minimisation carried out by Polak-Ribiere conjugate-gradient refinement, with the metal complex treated as a rigid group. Minimisation was continued until the RMS energy gradient was less than 0.2 kJ $Å^{-1}$ mol^{-1}.

Results

Assignment of the oligonucleotide and metal complex resonances

The ^{1}H NMR resonances of the free d(CCGAGAATTCCGG)$_2$ have previously been assigned by Kalnik *et al.*,[15] who also established that the tridecanucleotide adopted a B-type double helical structure with the adenine base bulge being stacked within the duplex. The resonances of the free control dodecanucleotide and the metal complex-bound oligonucleotides were assigned from NOESY and DQFCOSY spectra according to well-established procedures.[24–26] The assignment of the resonances from the metal complexes was also obtained from analysis of NOESY and DQFCOSY spectra. For the diastereoisomers of the [{Ru(bpy)$_2$}(μ-bpm){Ru(Me$_2$bpy)$_2$}]$^{4+}$ complex, unambiguous assignment of the resonances could be made by the observation of NOEs from the Me$_2$bpy ligand to the bpy ligand. For the oligonucleotide-bound metal complex, the NOE from the H5 of the Me$_2$bpy to the H6 of the bpy ligand was used as the basis for the resonance assignments, as the H6 of the Me$_2$bpy ligand is coincident with the H5 of the bpy ligand. The remaining metal complex resonances were easily assigned in the DQFCOSY and NOESY spectra. As it was not possible to unambiguously distinguish between the HX and HX′ protons for the [{Ru(Me$_2$bpy)$_2$}$_2$(μ-bpm)]$^{4+}$ complex, the assignments were made by comparison to the [{Ru(bpy)$_2$}(μ-bpm)-{Ru(Me$_2$bpy)$_2$}]$^{4+}$ species.

Binding of ΔΔ-[{Ru(Me$_2$bpy)$_2$}$_2$(μ-bpm)]$^{4+}$ to d(CCGGAATTCCGG)$_2$

Fig. 2 shows the aromatic region of the ^{1}H NMR spectrum of the d(CCGAGAATTCCGG)$_2$ with added ΔΔ-[{Ru(Me$_2$bpy)$_2$}$_2$(μ-bpm)]$^{4+}$. Only one set of dodecanucleotide and metal complex resonances were observed upon addition of the metal complex, indicating that the binding kinetics are in the fast exchange regime (on the NMR time scale). By following the chemical shifts of the resonances from the metal complex throughout the titration with ΔΔ-[{Ru(Me$_2$bpy)$_2$}$_2$(μ-bpm)]$^{4+}$,

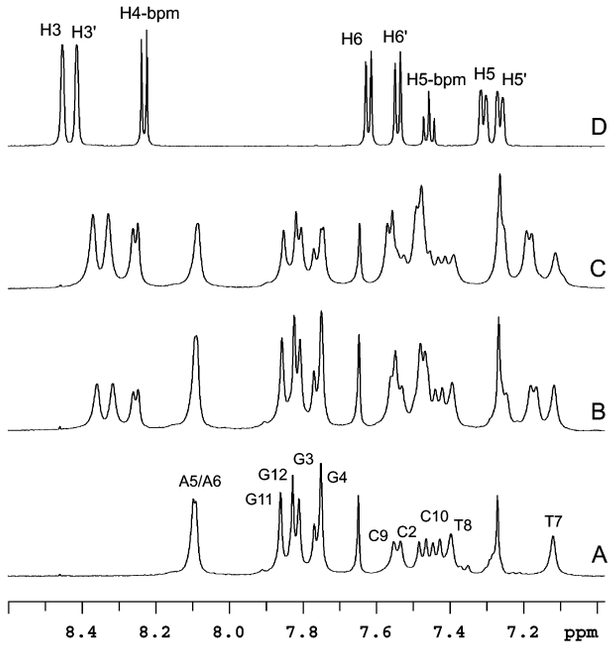

Fig. 2 ^{1}H NMR spectrum of the free d(CCGGAATTCCGG)$_2$ (1.2 mM) (A) and with added ΔΔ-[{Ru(Me$_2$bpy)$_2$}$_2$(μ-bpm)]$^{4+}$ at a metal complex to dodecanucleotide duplex ratio of 0.5 (B) and 1.0 (C) and the free metal complex (D) in 10 mM phosphate buffer (pH 7) containing 20 mM NaCl and 1 mM Na$_2$H$_2$EDTA at 25 °C.

the metal complex-d(CCGGAATTCCGG)$_2$ association constant was determined (using the equations given in the Experimental section) to be 4 × 10^3 M^{-1}, consistent with previous results.[10]

In NOESY spectra of the metal complex bound to the non-bulged dodecanucleotide (see Fig. 3), NOEs were observed between protons from the metal complex and H1′ and H4′ protons from the G_{12}, G_{11} and C_1 residues of the dodecanucleotide. In addition, weak intermolecular NOEs were also observed between the metal complex methyl protons and the dodecanucleotide A_6H2 proton. The combined NMR data

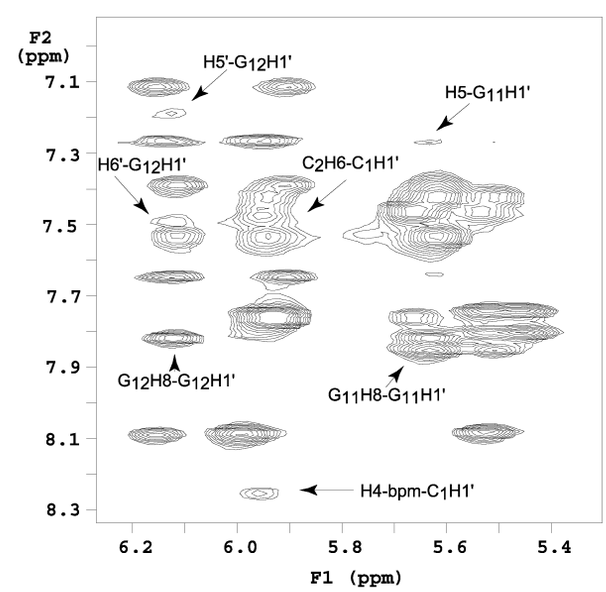

Fig. 3 Expansion of the NOESY spectrum (300 ms mixing time) of ΔΔ-[{Ru(Me$_2$bpy)$_2$}$_2$(μ-bpm)]$^{4+}$ and d(CCGGAATTCCGG)$_2$ (1.2 mM), at a metal complex to duplex ratio of 1.0 at 25 °C. The expansion shows the NOE connectivities from the dodecanucleotide base and metal complex aromatic protons (7.0 to 8.3 ppm) to the dodecanucleotide sugar H1′ protons (5.4 to 6.2 ppm). The NOE cross-peaks between the H5, H5′, H6′ and H4-bpm metal complex protons and the dodecanucleotide C_1, G_{11} and G_{12} protons are indicated.

Table 1 Chemical shifts (ppm) of the non-exchangeable protons of d(CCGAGAATTCCGG)$_2$ in 10 mM phosphate buffer containing 20 mM NaCl and 1 mM Na_2H_2EDTA at 25 °C. Numbers in parentheses indicate the difference between the chemical shift of the ΔΔ-[{Ru(Me$_2$bpy)$_2$}$_2$(μ-bpm)]$^{4+}$ bound and free tridecanucleotide resonances

Base	H8/H6	AH2	H1′	H2′	H2″	H3′	H4′
C_1	7.80		6.02	2.07	2.53	4.69	4.13
	(0.00)		(0.01)	(−0.02)	(−0.01)	(−0.01)	(0.01)
C_2	7.52		5.62	1.94	2.25	4.82	4.07
	(−0.01)		(−0.03)	(−0.02)	(−0.02)	(0.02)	(−0.02)
G_3	7.90		5.64	2.42	2.68	4.97	4.25
	(−0.13)		(−0.18)	(−0.19)	(−0.22)	(−0.07)	(−0.08)
A_4	7.92	7.62	5.66	2.44	2.52	4.90	4.26
	(0.08)	(0.05)	(0.10)	(0.09)	(0.01)	(−0.01)	(−0.11)
G_5	7.75		5.30	2.54	2.60	4.93	4.28
	(0.01)		(−0.08)	(0.01)	(0.00)	(−0.03)	(−0.08)
A_6	8.06	7.32	5.95	2.65	2.86	5.01	4.42
	(0.00)	(0.00)	(0.01)	(−0.03)	(0.01)	(−0.01)	(0.04)
A_7	8.11	7.71	6.19	2.58	2.91	5.01	4.48
	(0.00)	(0.01)	(−0.01)	(−0.04)	(−0.02)	(−0.01)	(−0.02)
T_8	7.14		5.92	1.97	2.56	4.82	4.20
	(0.00)		(−0.01)	(0.00)	(−0.02)	(0.02)	(−0.01)
T_9	7.41		6.08	2.15	2.55	4.91	4.19
	(0.00)		(−0.01)	(−0.02)	(−0.02)	(0.00)	(−0.01)
C_{10}	7.52		6.19	1.94	2.16	4.82	4.20
	(0.00)		(−0.04)	(−0.02)	(0.07)	(0.02)	(−0.02)
C_{11}	7.70		5.51	2.17	2.35	4.86	4.13
	(0.00)		(−0.10)	(−0.04)	(−0.05)	(−0.02)	(−0.10)
G_{12}	7.89		5.65	2.67	2.69	4.97	4.19
	(−0.01)		(−0.01)	(−0.04)	(−0.02)	(−0.02)	(−0.02)
G_{13}	7.86		6.17	2.56	2.37	4.66	4.19
	(−0.02)		(−0.01)	(−0.01)	(−0.02)	(0.01)	(−0.02)

indicate that the metal complex binds weakly to the non-bulged oligonucleotide at the terminal GG/CC base-pairs, and to some extent at the central AATT sequence.

Binding of ΔΔ-[{Ru(Me$_2$bpy)$_2$}$_2$(μ-bpm)]$^{4+}$ to d(CCGAGAATTCCGG)$_2$

Fig. 4 shows the aromatic region of the ^{1}H NMR spectrum of the bulged tridecanucleotide d(CCGAGAATTCCGG)$_2$, and the tridecanucleotide with added ΔΔ-[{Ru(Me$_2$bpy)$_2$}$_2$-(μ-bpm)]$^{4+}$. Only one set of tridecanucleotide and metal complex resonances was observed upon addition of the metal complex. However, there was considerable broadening of the resonances from the metal complex upon binding to the tridecanucleotide, indicating that the binding kinetics are in the intermediate to fast exchange regime.

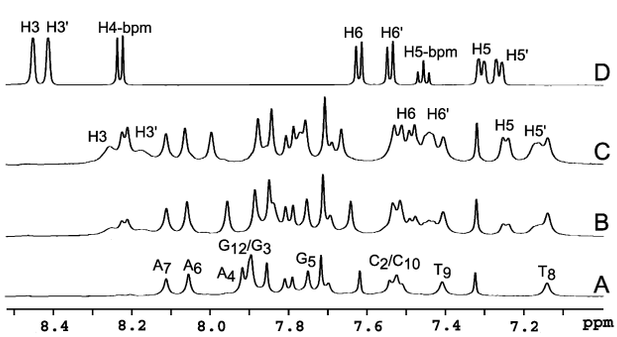

Fig. 4 ^{1}H NMR spectrum of the free d(CCGAGAATTCCGG)$_2$ (1.1 mM) (A) and with added ΔΔ-[{Ru(Me$_2$bpy)$_2$}$_2$(μ-bpm)]$^{4+}$ at a metal complex to tridecanucleotide duplex ratio of 0.5 (B) and 1.0 (C) and the free metal complex (D) in 10 mM phosphate buffer (pH 7) containing 20 mM NaCl and 1 mM Na_2H_2EDTA at 25 °C.

Addition of the metal complex only induced significant changes (≥0.05 ppm) in chemical shift for resonances from the G_3, A_4, G_5, C_{10} and C_{11} residues from the tridecanucleotide (see Table 1). This suggests that the metal complex is binding at or near the adenine bulge site. The H3/H3′, H5/H5′ and H6/H6′ resonances from the metal complex exhibited significant upfield shifts upon binding (see Fig. 4 and Table 2). However, as the chemical shifts of these metal complex resonances were the same at all points in the titration (±0.01 ppm) it can be concluded that the metal complex binds essentially stoichiometrically at each metal complex-to-tridecanucleotide duplex ratio (R) up to $R = 2$. This conclusion is further supported by the observation of the completely linear change as a function of the added metal complex in the chemical shift of the tridecanucleotide resonances that exhibited large shifts throughout the titration (*e.g.* G_3H1′). Given that the metal complex binds stoichiometrically, an association constant of $\geq 10^5$ M^{-1} can be calculated because the concentrations of the metal complex and tridecanucleotide are known. This indicates that the metal complex binds to the tridecanucleotide with, at the very least, one order of magnitude greater affinity than it did to the corresponding non-bulged dodecanucleotide, or either the CCGG or AAT sequences in other standard duplex DNA.[10]

In spectra of both the free and metal complex bound (for R = 1.0, 1.5 and 2) tridecanucleotide recorded in 90% H_2O/10% D_2O, five imino resonances were observed (see Fig. 5). This indicates that the duplex structure is maintained upon metal complex binding, with only the terminal residues not forming a stable base-pair.

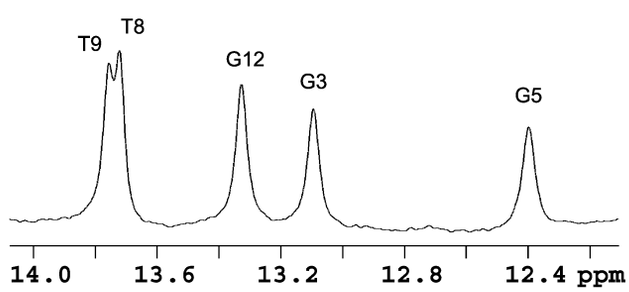

Fig. 5 ^{1}H NMR spectrum of the imino protons of d(CCGAGA-ATTCCGG)$_2$ with added ΔΔ-[{Ru(Me$_2$bpy)$_2$}$_2$(μ-bpm)]$^{4+}$, at a metal complex to duplex ratio of 1.5 in 10 mM phosphate buffer (pH 7) containing 20 mM NaCl and 1 mM Na_2H_2EDTA at 5 °C.

NOESY experiments were recorded in order to obtain a more detailed picture of the metal complex-tridecanucleotide binding. Fig. 6 shows an expansion of the NOESY spectrum of

Table 2 Chemical shift changes (ppm) for the resonances from ΔΔ-[{Ru(Me_2bpy)$_2$}$_2$(μ-bpm)]$^{4+}$ upon oligonucleotide binding, at a metal complex to duplex ratio of 1.0 in 10 mM phosphate buffer containing 20 mM NaCl and 1 mM Na_2H_2EDTA at 25 °C

Metal complex protons	Free *rac*-[{Ru(Me_2bpy)$_2$}$_2$(μ-bpm)]$^{4+}$	Control dodecamer binding	Bulge tridecamer binding
H3	8.45	8.37	8.26
H3′	8.42	8.33	8.18
H4-bpm	8.23	8.25	8.22
H6	7.62	7.56	7.49
H6′	7.54	7.48	7.45
H5-bpm	7.46	7.47	7.44
H5	7.31	7.26	7.25
H5′	7.26	7.18	7.17

Table 3 NOE Cross-peaks observed between ΔΔ-[{Ru(Me_2bpy)$_2$}$_2$-(μ-bpm)]$^{4+}$ and d(CCGAGAATTCCGG)$_2$, at a metal complex to duplex ratio of 1.0, in 10 mM phosphate buffer (pH 7) containing 20 mM NaCl and 1 mM Na_2H_2EDTA at 25 °C

Metal complex proton	Tridecanucleotide protons
H4-bpm	G_5H1′, C_{11}H1′, G_3H4′, G_5H4′, C_{11}H4′
H5-bpm	G_5H1′, C_{11}H1′
H5	G_5H4′, G_5H5′/H5″, C_{11}H5′/H5″
H5′	G_3H1′, A_4H1′, G_3H4′, G_3H5′/H5″
Methyl	G_3H1′, A_4H1′, C_{10}H1′

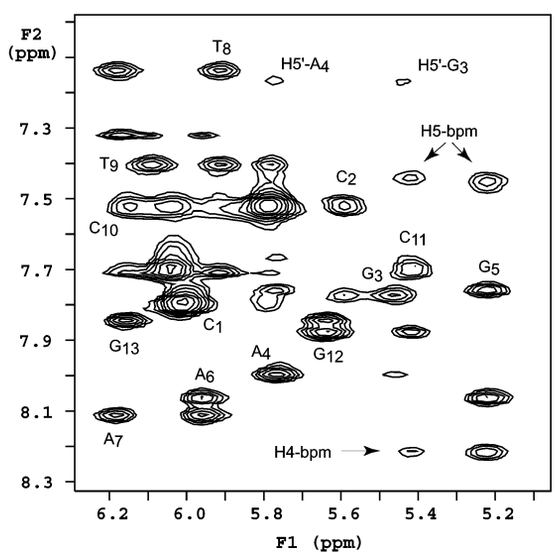

Fig. 6 Expansion of the NOESY spectrum (300 ms mixing time) of ΔΔ-[{Ru(Me_2bpy)$_2$}$_2$(μ-bpm)]$^{4+}$ and d(CCGAGAATTCCGG)$_2$ (1.1 mM), at a metal complex to duplex ratio of 1.0 at 25 °C. The expansion shows the NOE connectivities from the tridecanucleotide base and metal complex aromatic protons (7.0 to 8.3 ppm) to the tridecanucleotide sugar H1′ protons (5.1 to 6.2 ppm). The assignment of each base H1′ proton and the intermolecular NOEs between the metal complex and tridecanucleotide are indicated.

the metal complex bound tridecanucleotide at $R = 1$. In addition to the intraduplex NOEs expected for a B-type DNA duplex, a variety of intermolecular NOEs were observed between the metal complex and the tridecanucleotide. In particular, relatively strong NOEs are observed between the H4 and H5 bpm protons and the G_5 and C_{11} H1′ sugar protons. In addition, a number of other intermolecular NOEs are observed (see Table 3), including NOEs from the A_4H1′ proton to the H5′ and methyl protons of the metal complex. As the sugar H1′ protons are located in the DNA minor groove, the data indicate that the metal complex binds at the adenine bulge site in the minor groove. The observed pattern of intermolecular NOE's suggest that the metal complex binds at the adenine bulge site by lying diagonally across the minor groove between the G_5 residue on one strand and the C_{11} residue on the other strand.

Binding of ΔΔ-[{Ru(bpy)$_2$}(μ-bpm){Ru(Me_2bpy)$_2$}]$^{4+}$ to d(CCGAGAATTCCGG)$_2$

As previously observed for the binding of the ΔΔ-[{Ru-(Me_2bpy)$_2$}$_2$(μ-bpm)]$^{4+}$ complex, only one set of resonances was observed upon addition of ΔΔ-[{Ru(bpy)$_2$}(μ-bpm)-{Ru(Me_2bpy)$_2$}]$^{4+}$ to the tridecanucleotide (see Fig. 7). Again,

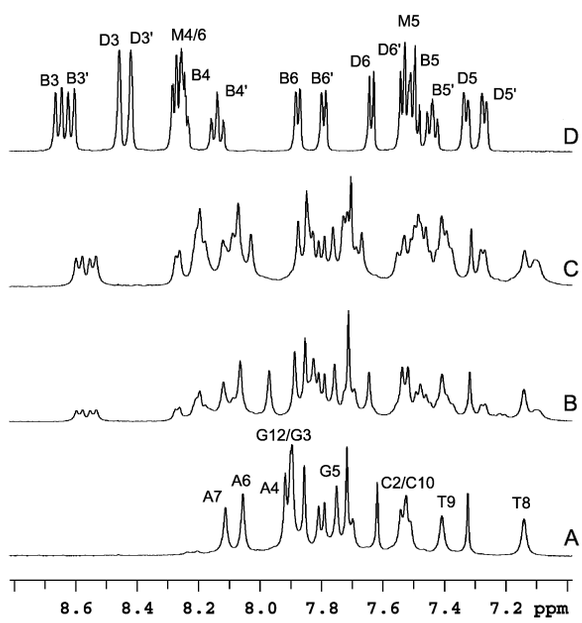

Fig. 7 ^{1}H NMR spectrum of the free d(CCGAGAATTCCGG)$_2$ (1.2 mM) (A) and with added ΔΔ-[{Ru(bpy)$_2$}(μ-bpm){Ru(Me_2bpy)$_2$}]$^{4+}$, at a metal complex to tridecanucleotide duplex ratio of 0.45 (B) and 1.0 (C) and the free metal complex (D) in 10 mM phosphate buffer (pH 7) containing 20 mM NaCl and 1 mM Na_2H_2EDTA at 25 °C. The notation D refers to the Me_2bpy ligand, B to the bpy ligand and M to the bpm ligand.

some broadening of several resonances from the metal complex was observed. Of the metal complex peaks that were clearly resolved, the Me_2bpy protons appeared to have exhibited the largest increase in line widths. Upfield shifts were observed for the resonances of all metal complex protons (see Table 4), but the resonances from the Me_2bpy ligand generally exhibited much larger upfield shifts than the resonances from the bpy ligand upon the binding of the metal complex to the tridecanucleotide. The chemical shift of the added metal complex remained constant throughout the titration, indicating that an association constant of $\geq 10^5$ M^{-1} may be assigned to the binding.

Addition of ΔΔ-[{Ru(bpy)$_2$}(μ-bpm){Ru(Me_2bpy)$_2$}]$^{4+}$ induced significant changes in chemical shift for the resonances from the base and sugar protons surrounding the bulge site (see Table 5). This indicates that the ΔΔ-[{Ru(bpy)$_2$}(μ-bpm)-{Ru(Me_2bpy)$_2$}]$^{4+}$ complex binds at the bulge site in a similar fashion to the symmetric ΔΔ-[{Ru(Me_2bpy)$_2$}$_2$(μ-bpm)]$^{4+}$ complex.

Table 4 ^{1}H NMR Chemical shifts (ppm) of the free ΔΔ-[{Ru(bpy)$_2$}(μ-bpm){Ru(Me$_2$bpy)$_2$}]$^{4+}$ and the tridecanucleotide bound metal complex in 10 mM phosphate buffer (pH 7) containing 20 mM NaCl and 1 mM Na_2H_2EDTA at 25 °C

Metal complex proton	Free metal complex	Tridecamer bound metal complex	Change in shift upon binding
Me$_2$bpy			
H3	8.46	8.18	−0.28
H3′	8.42	8.08	−0.34
H5	7.33	7.28	−0.05
H5′	7.27	7.11	−0.16
H6	7.64	7.48	−0.16
H6′	7.54	7.38	−0.16
bpy			
H3	8.66	8.59	−0.07
H3′	8.61	8.54	−0.07
H4	8.25	8.21	−0.04
H4′	8.14	8.10	−0.04
H5	7.49	7.48	−0.01
H5′	7.44	7.41	−0.03
H6	7.87	7.84	−0.03
H6′	7.79	7.72	−0.07
bpm			
H4/6-bpm	8.28	8.27	−0.01
H5-bpm	7.49	7.46	−0.03

Table 5 Changes in the chemical shifts (ppm) of the non-exchangeable protons of d(CCGAGAATTCCGG)$_2$ in 10 mM phosphate buffer containing 20 mM NaCl and 1 mM Na_2H_2EDTA at 25 °C upon the addition of $R = 1$ ΔΔ-[{Ru(bpy)$_2$}(μ-bpm){Ru(Me$_2$bpy)$_2$}]$^{4+}$

Base	H8/H6	AH2	H1′	H2′	H2″	H3′	H4′
C_1	0.00		0.01	−0.01	−0.01	0.00	0.00
C_2	0.00		−0.04	−0.02	−0.04	0.01	−0.02
G_3	−0.17		−0.23	−0.21	−0.25	−0.07	−0.09
A_4	0.11	0.05	0.13	0.10	0.02	−0.01	−0.14
G_5	0.01		−0.11	0.02	−0.04	−0.04	−0.10
A_6	0.01	−0.01	0.01	−0.04	0.02	−0.02	0.03
A_7	0.01	−0.01	0.01	−0.01	−0.01	−0.02	−0.03
T_8	0.00		−0.01	0.00	−0.03	0.01	−0.02
T_9	0.00		0.01	−0.02	−0.01	0.00	−0.03
C_{10}	0.03		−0.03	−0.02	−0.02	0.03	−0.03
C_{11}	0.00		−0.10	−0.04	−0.06	−0.02	−0.11
G_{12}	−0.02		−0.03	0.00	−0.02	−0.02	−0.02
G_{13}	−0.01		−0.01	−0.01	−0.01	0.00	−0.02

NOESY spectra of ΔΔ-[{Ru(bpy)$_2$}(μ-bpm){Ru(Me$_2$bpy)$_2$}]$^{4+}$ with the tridecanucleotide were recorded to obtain a more detailed picture of the metal complex binding to the adenine bulge site (see Fig. 8). As several tridecanucleotide and metal complex proton resonances were coincident at 25 °C, NOESY spectra were also recorded at 15 °C. A similar pattern of NOEs was observed between the ΔΔ-[{Ru(bpy)$_2$}(μ-bpm){Ru(Me$_2$bpy)$_2$}]$^{4+}$ and tridecanucleotide protons (see Table 6) as that detected for the ΔΔ-[{Ru(Me$_2$bpy)$_2$}$_2$(μ-bpm)]$^{4+}$ binding. Interestingly, only a few weak intermolecular NOEs were observed between the tridecanucleotide and the bpy protons. The NOESY spectra were consistent with the tridecanucleotide maintaining the basic B-type DNA conformation upon the binding of the ΔΔ-[{Ru(bpy)$_2$}(μ-bpm){Ru(Me$_2$bpy)$_2$}]$^{4+}$ complex. NOEs were observed from each base H8/H6 resonance to its own sugar H1′/H2′/H2″ protons as well as to the H1′/H2′/H2″ protons of the sugar of the nucleotide residue in the 5′-direction.[24–27] Furthermore, the NOEs from each base H8/H6 proton to its own H2′ proton was larger than the NOE to the H2′ proton on the 5′-sugar.[26,27] However, some minor conformational differences were apparent from the observed pattern of intraduplex NOEs. In particular, the NOE observed between the A_4H8 and G_3H1′ protons for both the free and ΔΔ-[{Ru(bpy)$_2$}(μ-bpm){Ru(Me$_2$bpy)$_2$}]$^{4+}$-bound tridecanucleotide is significantly weaker than other corresponding H8/H6 to the H1′ of the 5′-sugar.

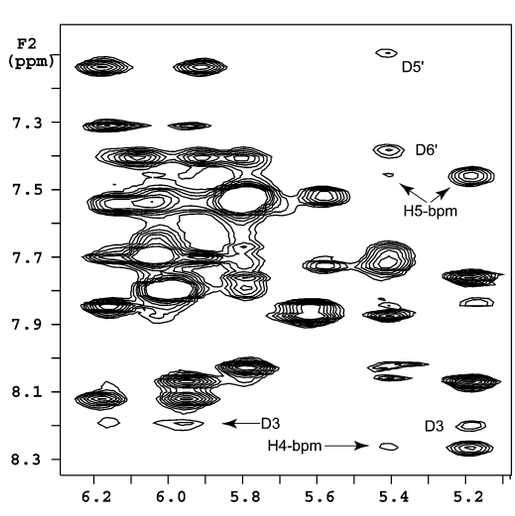

Fig. 8 Expansion of the NOESY spectrum (300 ms mixing time) of ΔΔ-[{Ru(bpy)$_2$}(μ-bpm){Ru(Me$_2$bpy)$_2$}]$^{4+}$ and d(CCGAGAATTCCGG)$_2$ (1.2 mM), at a metal complex to duplex ratio of 1.0 at 25 °C. The expansion shows the NOE connectivities from the tridecanucleotide base and metal complex aromatic protons (7.1 to 8.3 ppm) to the tridecanucleotide sugar H1′ protons (5.1 to 6.2 ppm). The notation D refers to the Me$_2$bpy ligand protons. Intermolecular NOEs from the H4- and H5-bpm to the G_5 and C_{11}H1′; D5′ and D6′ to the C_{11}H1′; and D3 to the G_5, A_6 and C_{10}H1′ are shown.

Table 6 NOE Cross-peaks observed between ΔΔ-[{Ru(bpy)$_2$}(μ-bpm){Ru(Me$_2$bpy)$_2$}]$^{4+}$ and d(CCGAGAATTCCGG)$_2$, at a metal complex to duplex ratio of 1.0, in 10 mM phosphate buffer (pH 7) containing 20 mM NaCl and 1 mM Na$_2$H$_2$EDTA at 25 °C. The letters in parentheses indicate the relative strength of the observed NOE; S = strong; M = medium; and W = weak

Metal complex proton	Tridecanucleotide protons
H4/6-bpm	G_5H1′ (S), C_{11}H1′ (W), G_5H4′ (S), C_{11}H4′ (M)
H5-bpm	G_5H1′ (S), C_{11}H1′ (W), G_5H4′ (S)
H5′-Me$_2$bpy	C_{11}H1′ (W)
H5-Me$_2$bpy	C_{11}H4′ (M), G_5H4′ (M)
H6′-Me$_2$bpy	C_{11}H1′ (M), C_{11}H4′ (M)
H3-Me$_2$bpy	G_5H1′ (M), A6H1′ (W), C_{10}H1′ (W), G_5H4′ (S), C_{11}H4′ (M)
H3-bpy	G_5H4′ (W)
H3′-bpy	G_5H4′ (W)
Methyl	G_5H4′ (S), C_{11}H4′ (M)

ΔΔ-[{Ru(bpy)$_2$}(μ-bpm){Ru(Me$_2$bpy)$_2$}]$^{4+}$ Binding model

As only exchange-averaged resonances were observed from the ΔΔ-[{Ru(bpy)$_2$}(μ-bpm){Ru(Me$_2$bpy)$_2$}]$^{4+}$ complex and the tridecanucleotide, the NMR data did not allow the determination of a quantitative structure. However, several simple HyperChem binding models were constructed to examine the proposed ΔΔ-[{Ru(bpy)$_2$}(μ-bpm){Ru(Me$_2$bpy)$_2$}]$^{4+}$ binding at the bulge site of the tridecanucleotide. The metal complex was manually docked in the tridecanucleotide minor groove at the bulge site. The ruthenium centre containing the Me$_2$bpy ligands was positioned more deeply within the groove, consistent with the NMR results, with the Ru(bpy)$_2$ moiety projecting out of the groove (due to the curvature of the sugar phosphate backbone). The system was then energy minimised with the metal complex being treated as a rigid group.

Fig. 9 shows a representative binding model that is consistent with the observed metal complex-tridecanucleotide NOEs. The double helical structure of the tridecanucleotide is maintained upon metal complex binding and the single adenine base bulge remains within the stacked bases, consistent with the NMR data. In the minimised model of the free and metal complex-bound tridecanucleotide, the three purine bases at the bulge site appear to stack on each other with the two cytosine residues slightly "wedged out" with their base-paired guanine residues, consistent with the original proposal of Kalnik *et al.*[15] In addition, the distance between the A_4H8 and G_3H1′ protons is 4.3 Å (compared to the normal distance of about 3.6 Å)[24] consistent with the weak NOE observed between these protons. Of note in the binding model is the significant widening of the minor groove to accommodate the ΔΔ-[{Ru(bpy)$_2$}(μ-bpm){Ru(Me$_2$bpy)$_2$}]$^{4+}$ complex. Indeed, the minor groove is almost wide enough to accommodate the axial 4-methyl groups on the Me$_2$bpy ligands of the metal complex, where the distance between the two methyl carbon atoms is 12.3 Å.

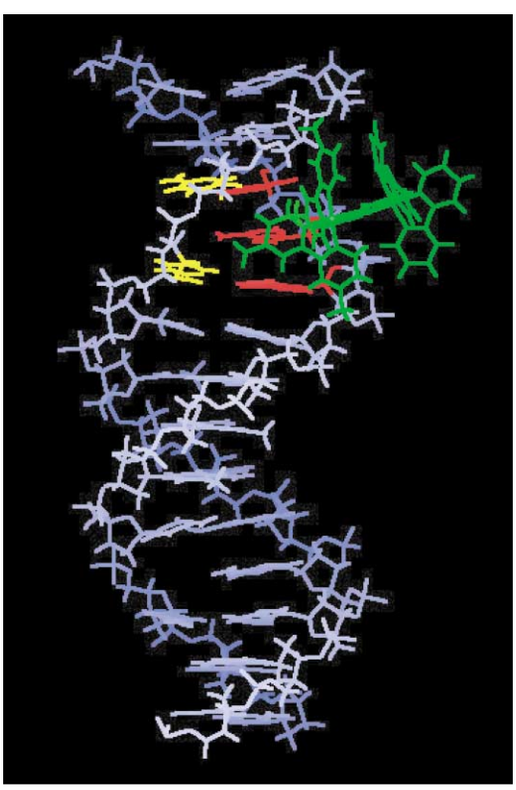

Fig. 9 Molecular model of ΔΔ-[{Ru(bpy)$_2$}(μ-bpm){Ru(Me$_2$bpy)$_2$}]$^{4+}$ bound to d(CCGAGAATTCCGG)$_2$ generated using HyperChem. The model of the tridecanucleotide duplex was generated in HyperChem and the metal complex inserted into the minor groove at the adenine bulge site. Energy minimisation of the tridecanucleotide was then carried out to convergence. The G_3, A_4 and G_5 residues are coloured red, while the C_{10} and C_{11} residues are coloured yellow.

Discussion

Synthesis and separation of stereoisomers of [{Ru^B(bpy)$_2$}(μ-bpm){Ru^D(Me$_2$bpy)$_2$}]$^{4+}$

A full description of the synthesis of [{Ru(bpy)$_2$}(μ-bpm){Ru(Me$_2$bpy)$_2$}]$^{4+}$ and the separation of the four stereoisomers will be given elsewhere,[28] but the procedure involved in the isolation of the ΔΔ form is given here.

The synthesis of [{Ru(bpy)$_2$}(μ-bpm){Ru(Me$_2$bpy)$_2$}]$^{4+}$ was undertaken in a non-stereoselective manner: [Ru(bpy)$_2$bpm]$^{2+}$ and [Ru(Me$_2$bpy)$_2$(CO)$_2$]$^{2+}$ were heated in 2-methoxyethanol after the addition of TMNO to yield a mixture of all possible stereoisomers. Due to the non-equivalence of the two ends of the dinuclear complex — *i.e.* [{Ru(pp)$_2$}(μ-bpm){Ru(pp′)$_2$}]$^{4+}$ where pp ≠ pp′ — both "*meso*"[29] and *rac* diastereoisomers exist as a pair of enantiomers, ΔΛ/ΛΔ and ΔΔ/ΛΛ, respectively.

The separation of the "*meso*" and *rac* diastereoisomers, and resolution of the *rac* form into the ΔΔ- and ΛΛ-enantiomers, were achieved using a single chromatographic step. The CD spectra of ΔΔ- and ΛΛ-[{Ru(bpy)$_2$}(μ-bpm){Ru(Me$_2$bpy)$_2$}]$^{4+}$ are given in the ESI (Fig. S1).

As noted above, dinuclear ligand-bridged complexes that possess non-equivalent metal centres give rise to a "*meso*" form that will consist of two enantiomers — designated $\Delta^B\Lambda^D$ and $\Lambda^B\Delta^D$ where the superscripts B and D represent the centre with bpy and Me$_2$bpy ligands, respectively. Enantiomers of this form have not been resolved previously and inspection reveals it to be a challenging prospect. The resolution was achieved in this work and will be reported subsequently,[28] as the "*meso*" forms of the complex were not used in the present binding studies.

Characterisation of the diastereoisomers of [{Ru(bpy)$_2$}(μ-bpm){Ru(Me$_2$bpy)$_2$}]$^{4+}$ was achieved by NMR spectroscopy. Both diastereoisomers possess C_2 point group symmetry, with the C_2 axis running through both metal atoms and bisecting the bridging ligand. As a consequence, each pair of bpy and Me$_2$bpy ligands gives rise to only one set of resonances. In addition, the two halves of the bridging ligand are also equivalent. Characterisation was achieved by performing COSY experiments, and the individual pyridyl rings of the bpy, Me$_2$bpy and bpm ligands could be identified.

Binding of dinuclear metal complexes to the oligonucleotides

The binding of the dinuclear ruthenium(II) complex ΔΔ-$[\{Ru(Me_2bpy)_2\}_2(\mu\text{-bpm})]^{4+}$ to an oligonucleotide containing a single adenine bulge and the corresponding control, non-bulged, oligonucleotide has been studied by NMR spectroscopy. Consistent with an earlier study, the metal complex bound to the non-bulged dodecanucleotide weakly in the DNA minor groove and predominantly at the terminal CC/GG base-pairs.[10,16] Alternatively, for the adenine bulge-containing tridecanucleotide, the NMR data indicated that the metal complex bound selectively at the bulge site and with a considerably greater affinity than that observed for the binding to the non-bulged oligonucleotide. This conclusion is consistent with the observation that the similar dinuclear complex $[\{Ru(phen)_2\}_2(\mu\text{-HAT})]^{4+}$ interacted only weakly with double-stranded DNA but relatively strongly with partially-denatured DNA.[8]

In order to obtain a simple binding model, the binding of the non-symmetrical ruthenium(II) complex ΔΔ-$[\{Ru(bpy)_2\}(\mu\text{-bpm})\{Ru(Me_2bpy)_2\}]^{4+}$ to the bulge containing tridecanucleotide was studied. Again, this non-symmetrical dinuclear ruthenium(II) complex selectively bound the tridecanucleotide at the bulge site. As the changes in the chemical shift for the tridecanucleotide and metal complex resonances and the observed pattern of metal complex-oligonucleotide NOEs were very similar to that observed for the symmetric ΔΔ-$[\{Ru(Me_2bpy)_2\}_2(\mu\text{-bpm})]^{4+}$ complex, it is concluded that both metal complexes bind at the bulge site in a similar fashion. Interestingly, the NMR data suggest the ruthenium centre containing the more bulky Me_2bpy ligands is positioned more deeply within the groove, as shown in the binding model. It is not clear why this should be; however, it is possible that the NOE data could be affected by the different rates of exchange between the two possible binding orientations and the free metal complex.

Despite the relative bulky nature of the metal complexes, they bound at the bulge site in the DNA minor groove, rather than the significantly wider major groove. The results of this and an earlier study[10] indicate that the dinuclear complexes also bind "normal" duplex DNA in the minor groove. However, the metal complexes bind the adenine bulge site with considerably greater affinity. This is presumably due to the significant widening of the minor groove that occurs at the bulge site and allows the metal complex to bind more deeply in the groove. The minor groove at the bulge site of the free tridecanucleotide is not significantly wider than that of "normal" duplex DNA. This indicates that the wide minor groove width for the metal complex-bound tridecanucleotide is due to an increased flexibility of the local DNA structure, rather than an inherent feature of a single base bulge sequence. The rational design of new DNA binding agents requires an understanding of the molecular interactions involved in sequence selective DNA recognition. Most studies have primarily concentrated on direct read-out mechanisms, the matching of hydrogen-bonds, electrostatic and van der Waals interactions between the functional groups of the small molecule and the particular DNA sequence. This strategy has led to the successful design of a variety of sequence selective binding agents.[30–32] However, an aspect of DNA recognition which has been less extensively studied is that of sequence dependent flexibility. The ability of particular sequences to undergo conformational distortions in order to optimise the binding of small ligand molecules may be an important factor in sequence specific DNA recognition.

In conclusion, the results of this study have demonstrated that the metal complexes ΔΔ-$[\{Ru(Me_2bpy)_2\}_2(\mu\text{-bpm})]^{4+}$ and ΔΔ-$[\{Ru(bpy)_2\}(\mu\text{-bpm})\{Ru(Me_2bpy)_2\}]^{4+}$ specifically bind at an adenine bulge site in a segment of DNA. In addition, the metal complex binds at the bulge site with an affinity considerably greater than was observed for the binding at sites on standard duplex DNA. As complexes such as $[\{Ru(phen)_2\}_2(\mu\text{-HAT})]^{4+}$ are also luminescent when tightly bound to DNA,[8] the results presented here suggest that non-intercalating dinuclear complexes may be excellent diagnostic agents for DNA bulged sequences.

Acknowledgements

We thank the Australian Research Council for financial support.

References and notes

1 A. M. Pyle and J. K. Barton, in *Progress in Inorganic Chemistry*, S. J. Lippard, ed., Wiley Interscience, New York, 1990, vol. 38, pp. 413–475.
2 B. Nordén, P. Lincoln, B. Akerman and E. Tuite, *Met. Ions Biol. Syst.*, 1996, **33**, 177–252.
3 K. E. Erkkila, D. T. Odom and J. K. Barton, *Chem. Rev.*, 1999, **99**, 2777–2795.
4 B. Önfelt, P. Lincoln and B. Nordén, *J. Am. Chem. Soc.*, 2001, **123**, 3630–3637.
5 P. Lincoln and B. Nordén, *Chem. Commun.*, 1996, 2145–2146.
6 X.-H. Zou, B.-H. Ye, H. Li, J.-G. Liu, Y. Xiong and L.-N. Ji, *J. Chem. Soc., Dalton Trans.*, 1999, 1423–1428.
7 F. M. O'Reilly and J. M. Kelly, *J. Phys. Chem. B*, 2000, **104**, 7206–7213.
8 O. Van Gijte and A. Kirsch-De Mesmaeker, *J. Chem. Soc., Dalton Trans.*, 1999, 951–956.
9 A. Brodkorb, A. Kirsch-De Mesmaeker, T. J. Rutherford and F. R. Keene, *Eur. J. Inorg. Chem.*, 2001, 2151–2160.
10 F. M. Foley, F. R. Keene and J. G. Collins, *J. Chem. Soc., Dalton Trans.*, 2001, 2968–2974.
11 D. M. J. Lilley, *Proc. Natl. Acad. Sci. USA*, 1995, **92**, 7140–7142.
12 K. Nakatani, S. Sando and I. Saito, *J. Am. Chem. Soc.*, 2000, **122**, 2172–2177.
13 C.-C. Chen, Y.-N. Kuo, K.-S. Chuang, C.-F. Luo and W. J. Wang, *Angew. Chem., Int. Ed.*, 1999, **38**, 1255–1257.
14 L. S. Kappen, Z. Xi and I. H. Goldberg, *Biochemistry*, 2001, **40**, 15378–15383.
15 M. W. Kalnik, D. G. Norman, P. F. Swann and D. J. Patel, *J. Biol. Chem.*, 1989, **264**, 3702–3712.
16 In our earlier paper (ref. 10), the designations of the enantiomers of the *rac* diastereoisomer of $[\{Ru(Me_2bpy)_2\}_2(\mu\text{-bpm})]^{4+}$ (ΔΔ and ΛΛ) were inadvertantly reversed, so that the results reported for the ΛΛ isomer were in fact those associated with the ΔΔ isomer.
17 N. C. Fletcher and F. R. Keene, *J. Chem. Soc., Dalton Trans.*, 1999, 683–689.
18 P. A. Anderson, G. B. Deacon, K. H. Haarmann, F. R. Keene, T. J. Meyer, D. A. Reitsma, B. W. Skelton, G. F. Strouse, N. C. Thomas, J. A. Treadway and A. H. White, *Inorg. Chem.*, 1995, **34**, 6145–6157.
19 T. Maniatis, E. F. Fritsch and J. Sambrook, *Molecular Cloning*, Cold Spring Harbor Laboratory, 1982.
20 D. J. States, R. A. Haberkorn and D. J. Ruben, *J. Magn. Reson.*, 1982, **48**, 286–292.
21 M. Piotto, V. Saudek and V. Sklenar, *J. Biomol. NMR*, 1992, **2**, 661–665.
22 M. Eriksson, M. Leijon, C. Hiort, B. Nordén and A. Graslund, *Biochemistry*, 1994, **33**, 5031–5040.
23 HyperChem Release 5.01 for Windows Molecular Modelling System, 1996, HyperCube Inc., Ontaria, Canada.
24 R. M. Scheek, R. Boelens, N. Russo, J. H. van Boom and R. Kaptein, *Biochemistry*, 1984, **23**, 1371–1376.
25 J. Feigon, W. Leupin, W. A. Denny and D. R. Kearns, *Biochemistry*, 1983, **22**, 5943–5951.
26 D. J. Patel, L. Shapiro and D. Hare, *J. Biol. Chem.*, 1986, **261**, 1223–1229.
27 K. Wuthrich, in *NMR of Proteins and Nucleic Acids*, John Wiley and Sons, New York, 1986.
28 B. T. Patterson, D. Richards, F. M. Foley, and F. R. Keene, unpublished work.
29 Although it is not strictly correct, the use of "*meso*" has been retained to describe the diastereoisomer in which the chiralities of the two metal centres are opposite.
30 C. R. Watts, S. M. Kerwin, G. L. Kenyon, I. D. Kuntz and D. A. Kallick, *J. Am. Chem. Soc.*, 1995, **117**, 9941–9950.
31 M. E. Parks, E. E. Baird and P. B. Dervan, *J. Am. Chem. Soc.*, 1996, **118**, 6147–6152.
32 B. P. Hudson, C. M. Dupureur and J. K. Barton, *J. Am. Chem. Soc.*, 1995, **117**, 9379–9380.